Selective-Delay Push-In Buffering Mechanism for QoS Provisioning in ATM Switching Nodes Loaded with ON-OFF Arrival Processes

Jongho Bang Nirwan Ansari Sirin Tekinay
Department of Electrical and Computer Engineering
New Jersey Institute of Technology
University Heights, Newark, NJ 07102, USA

Abstract

We propose a new space priority mechanism, and analyze its performance in a single CBR server. The arrival process is derived from the superposition of two types of traffics, each in turn results from the superposition of homogeneous ON-OFF sources that can be approximated by means of a two-state Markov Modulated Poisson Process (MMPP). The buffer mechanism enables the ATM layer to adapt the quality of the cell transfer to the QoS requirements and to improve the utilization of network resources. This is achieved by "Selective-Delaying and Pushing-In" (SDPI) cells according to the class they belong to. The scheme is applicable to schedule delay-tolerant non-real time traffic and delay-sensitive real time traffic. Analytical expressions for various performance parameters and numerical results are obtained. Simulation results in term of cell loss probability (CLP) conform with our numerical analysis.

1. Introduction

Several special mechanisms for buffer access have been proposed. They have been used to adapt the cell loss probability of a given class of traffic to the restrictions of the QoS needs of the corresponding service. These mechanisms allow a selective access to the buffer depending on the traffic class. In [1][2][3], the authors proposed a mechanism, called Push-Out, which guarantees the buffer access to a certain class of traffic if the queue is not full, and when it is full, the arriving cell can replace one with lower priority. The selection of the lowest priority cell to be rejected is done according to the chosen replacement algorithm. Other mechanisms proposed have lower performance but simpler buffer management, called Partial Buffer Sharing [4][5][6], which guarantees the buffer access to a class i cell if the buffer occupancy is less than a threshold, say, S_i. Hence, the highest priority class will be able to access the whole buffer. In general, these schemes are more flexible and more protective of high priority cells. However, this performance gain is always achieved only at the cost of a significant performance degradation of low priority cell loss probability.

Our simple consideration suggests that the traffic can be categorized into two basic classes: real time traffic (RTT) and non-real time traffic (NRTT). If a RTT ATM cell is not delivered to its destination within the maximum delay time, it would be dropped. The NRTT is more tolerant to delay, but has more stringent requirement for cell loss probability. Our model is based on the partial buffer sharing scheme. The buffer is partitioned by a threshold, set according to the maximum tolerant delay of RTT. In order to compensate for the disadvantage of partial buffer sharing scheme, we can give priority to the delay sensitive traffic over delay tolerant traffic selectively. We call such a proposed scheme, Selective-Delay Push-In (SDPI). In this paper, we make thorough study of the proposed space priority mechanism for the case of bursty traffic. The bursty source is modeled by the Markov Modulated Poisson Process (MMPP), because it is analytically tractable and possesses properties suitable for the approximation of complicated non-renewal processes. The rest of the paper is organized as follows. Section 2 describes the modeling of the space priority mechanism; Section 3 presents performance results; finally, some conclusions are drawn in Section 4.

2. Space priority mechanism

2.1. Source model

The MMPP has been extensively used for modeling arrival rates of point processes, because it qualitatively models the time-varying arrival rate and captures some of the

[0]This work was supported in part by the New Jersey Commission on Science and Technology via the NJ Center for Wireless Telecommunications and the NJ Commission on Higher Education via the NJI-TOWER Project.

0-7695-0951-7/01 $10.00 © 2001 IEEE

important correlations between the interarrival times while still remaining analytically tractable. The accuracy of MMPP in modeling an arrival process depends on which statistics of the actual process are used to determine its parameters. 2-state MMPP models [7][8][9] and 4-state MMPP models [10] have been used to approximate the superposition of ON-OFF sources. In [11], the superposition of ON-OFF sources is approximated by means of a 2-state MMPP using the Average Matching Technique. This technique provides good accuracy as compared to simulation results. In particular, the method weakly depends on the number of sources.

At first, assume that the superposition of N independent and homogeneous sources characterized by: 1) the peak bit rate, F_p; 2) the activity factor, p; 3) the mean burst length, L_B. With reference to the ATM MUX, denote C as the net output capacity, and thus $M = \lfloor C/F_p \rfloor$ indicates the maximum number of sources that can be accommodated in the MUX, assuming a peak bandwidth assignment. The superposition of N such sources results in a birth-death process. The states of this process are divided into two subsets [9]: 1) an overload (OL) region, comprising the states $M+1,\ldots,N$, where the cell emission rate exceeds the capacity C; 2) an underload (UL) region, consisting of the remaining states $0, \ldots, M$. Therefore, the two states of the approximated MMPP can be chosen so that one of them, called OL state, corresponding to the OL region, and the other, called UL state, associated with the UL region. Let π_j be the limiting probability that the number of active sources is j. Then π_j is given by the binomial distribution. $\pi_j=\binom{N}{j}p^j(1-p)^{N-j}$ where p is the activity factor of a source. Using the average matching procedure, the expression for the four parameters characterizing the MMPP can be determined.

We can adopt this Average Matching Technique for the superposition of independent heterogeneous ON-OFF, consisting of RTT and NRTT. In our case, the finite capacity can be shared by two kinds of traffic. A threshold is defined to separate the two state (Low and High) for each class of traffic. Let N_1 be the set of RTT with peak bit rate, $F_p(1)$, and N_2 be the set of NRTT with peak bit rate, $F_p(2)$. M_1 denotes the threshold which distinguishes the two states (low and high load) for RTT, and similarly, M_2 denotes the threshold which distinguishes the two states (low and high load) for NRTT.

$$M_1 = \left\lfloor \frac{N_1 C}{N_1 F_p(1) + N_2 F_p(2)} \right\rfloor \tag{1}$$

$$M_2 = \left\lfloor \frac{N_2 C}{N_1 F_p(1) + N_2 F_p(2)} \right\rfloor \tag{2}$$

Thus, we can divide into two states for each traffic. That is,

- For RTT
  low load region (Low(1)): $[0, 1, \ldots, M_1]$
  high load region (High(1)): $[M_1+1, \ldots, N_1]$

- For NRTT
  low load region (Low(2)): $[0, 1, \ldots, M_2]$
  high load region (High(2)): $[M_2 + 1, \ldots, N_2]$

Four parameters are required to represent the 2-state MMPP source of each traffic, as shown in Fig. 1, where $\gamma_{L1}(\gamma_{H1})$ is defined as the mean transition rate out of the Low load 1 (High load 1) state, and $\lambda_{L1}(\lambda_{H1})$ is the mean arrival rate of the Poisson process in the Low load 1 (High load 1) state for RTT, respectively. Similarly, $\gamma_{L2}(\gamma_{H2})$ is defined as the mean transition rate out of the Low load 2 (High load 2) state, and $\lambda_{L2}(\lambda_{H2})$ is the mean arrival rate of the Poisson process in the Low load 2 (High load 2) state for NRTT, respectively.

2.2 The SDPI mechanism

In general, the traffic can be categorized into two basic classes: RTT and NRTT. RTT has a limitation on the maximum delay time. If a RTT ATM cell is not delivered to its destination within the maximum delay time, it would be dropped. The RTT source may be of CBR or VBR type. The NRTT is more tolerant to delay, but has more stringent requirement for cell loss probability.

We modify Partial Buffer Sharing (PBS) scheme by giving other priority to the delay sensitive traffic over delay tolerant traffic selectively, and thus called selective-delay push-in (SDPI) scheme. With this scheme, ATM cells of delay tolerant traffics can be delayed in favor for cells of delay sensitive traffics. As illustrated in Fig. 2, when the buffer level is above the threshold, if there exist delay-tolerant cells within the threshold, an arriving delay-sensitive cell pushes out the latest arrived delay-tolerant cell and positions itself at the end of the buffer within the threshold. If no delay-tolerant cell is within the threshold, an arriving delay-sensitive cell is discarded.

2.3 SDPI Analysis

The multiplexer is modeled as a finite capacity single server queue where the arrival process is MMPP, and the service is deterministic. In our analysis, we make the similar assumptions as in [10], which deals with the analysis of only one traffic type, that significantly reduce the computational complexity involved in obtaining the stationary distributions at departure points: 1) the probability that the MMPP goes through multiple state transitions between successive departures is negligible, and 2) the state transitions occur at departure epochs, i.e., if a departure leaves the MMPP in state i, the cell arrival rate until the next departure is λ_i. Consider a queue using SDPI where the MMPP consists of K states denoted by i ($0 \le i \le K$-1), and the arrival rates and mean state durations are denoted by λ_i and μ_i, respectively. The characteristics of this system will be determined using an imbedded Markov chain approach. As in the ordinary M/G/1 queueing system, the service completion instants are the imbedded points of the underlying Markov chain. Therefore, a probability vector $\mathbf{\Pi}$ consists of $\pi_i(n_1, n_2)$ ($0 \le n_1 \le S_1, 0 \le n_2 \le S_2$, where S_2 is the total buffer size) which is defined by the probability that a departing cell leaves n_1 RTT cells and n_2 NRTT cells in the system while the MMPP is in state i. The total transition probability matrix of the imbedded Markov chain, denoted by $\mathbf{Q}$, is formed with K MMPP finite states and F finite buffer states. For example, consider the traffic shown in Fig. 1, where the RTT and NRTT can be aggregated resulting in a 4-state MMPP process (in this case, K=4). The K=4 states are $\{(L_1,L_2), (L_1,H_2), (H_1,L_2), (H_1,H_2)\}$. For a buffer with S_1=3 and S_2=6, there are F=22 finite buffer states corresponding to $\{\{n_1, n_2\} \mid n_1 + n_2 \le 6$ and $n_1 \le 3\}$. Thus,

$$\mathbf{Q} = \begin{bmatrix} Q_{0,0} & Q_{0,1} & \cdots & Q_{0,K-1} \\ Q_{1,0} & Q_{1,1} & \cdots & Q_{1,K-1} \\ \vdots & \vdots & \cdots & \vdots \\ Q_{K-1,0} & Q_{K-1,1} & \cdots & Q_{K-1,K-1} \end{bmatrix}, \tag{3}$$

where $Q_{j,i}$ is a submatrix, and each element of the submatrix, $Q_{j,i}((n_1,n_2),\ (n'_1,n'_2))$ ($0 \le j,i \le K$-1, $0 \le n_1, n'_1 \le S_1,\ 0 \le n_2, n'_2 \le S_2$) corresponds to a state transition probability. That is,

$Q_{j,i}((n_1,n_2),\ (n'_1,n'_2)) = P\{(n'_1,n'_2), j \mid (n_1,n_2), i\}$

where i is the present MMPP state, j is the next MMPP state, (n_1,n_2) is the present buffer state, and (n'_1,n'_2) is the next buffer state. The submatrix $Q_{j,i}$ can be obtained as follows. Denote A_i as the buffer state transition probability matrix of the departure point of our system at MMPP state i (with arrival rate λ_i and service time Δt). The transition probability submatrix $Q_{j,i}$ can be simply obtained by multiplying A_i by the probability that the MMPP will not change its state in Δt if $j = i$, or by the probability that the MMPP will change its state from j to i in Δt if $j \neq i$. Define $q_i(k,l)$ as the transition probability that k RTT cells and l NRTT cells can be positioned in the buffer during the service time (Δt) while the MMPP is in state i. Denote $q_i^1(k)$ as the probability of k arrivals of traffic type 1 (i.e., RTT) and $q_i^2(l)$ as the probability of l arrivals of traffic type 2 (i.e., NRTT) during the service time, respectively. Define $q_i^*(k,l)$ as the transition probability that more than k RTT cells and more than l NRTT cells are inserted to the buffer, but only k RTT cells and only l NRTT cells can be positioned in the buffer during the service time (Δt) due to the SDPI mechanism. Thus, $q_i(k,l) = q_i^1(k)q_i^2(l)$ where $q_i^1(k) = \frac{(\lambda_i^1 \Delta t)^k}{k!}e^{-(\lambda_i^1 \Delta t)}$ and $q_i^2(l) = \frac{(\lambda_i^2 \Delta t)^l}{l!}e^{-(\lambda_i^2 \Delta t)}$ and λ_i^1, λ_i^2 are the arrival rates for traffic type 1 and 2, respectively, and λ_i=λ_i^1+λ_i^2.

Since at most one cell is served between successive imbedded points, transitions from n_1 to $n'_1 < n_1 - 1$, from n_2 to $n'_2 < n_2 - 1$, and from n_1+n_2 to $n'_1+n'_2 < n_1+n_2-1$ are not possible.

Transitions to $n'_1 + n'_2 < S_2$ *and* $n'_1 < S_1$:

$$q_i(k,l) = q_i^1(k)q_i^2(l) \tag{4}$$

Transitions to boundary:

1. at $n'_1 + n'_2 < S_2$ and $n'_1 = S_1$,

$$q_i^*(k,l) = \sum_{n=k}^{\infty} q_i^1(n)q_i^2(l) \tag{5}$$

2. at $n'_1 + n'_2 = S_2$ and $n'_1 = S_1$,

$$q_i^*(k,l) = \sum_{n=k}^{\infty} q_i^1(n)q_i^2(l) + \sum_{n=k}^{\infty}\sum_{m=l+1}^{\infty} q_i^1(n)q_i^2(m)\frac{\binom{n}{k}\binom{m}{l}}{\binom{n+m}{n}} \tag{6}$$

3. at $n'_1 + n'_2 = S_2$ and $n'_1 < S_1$,

- $n'_1 = n_1 - 1$

$$q_i^*(k,l) = \sum_{m=l}^{\infty} q_i^1(k)q_i^2(m) + \sum_{n=k+1}^{\infty}\sum_{m=l}^{\infty} q_i^1(n)q_i^2(m)\frac{\binom{n}{k}\binom{m}{l}}{\binom{n+m}{n}} \tag{7}$$

- $n'_2 = n_2 - 1$

$$q_i^*(k,l) = \sum_{n=k}^{\infty} q_i^1(n)q_i^2(l) + \sum_{n=k}^{\infty}\sum_{m=l+1}^{\infty} q_i^1(n)q_i^2(m)\frac{\binom{n}{k}\binom{m}{l}}{\binom{n+m}{n}} \tag{8}$$

- *other cases*

$$q_i^*(k,l) = \sum_{n=k}^{\infty}\sum_{m=l}^{\infty} q_i^1(n)q_i^2(m)\frac{\binom{n}{k}\binom{m}{l}}{\binom{n+m}{n}} \quad (9)$$

Define the stationary probability vector $\mathbf{\Pi}$ as

$$\mathbf{\Pi} = \{\pi_0(0,0),...,\pi_0(S_1,S_2-S_1),\pi_1(0,0),..., ...,\pi_{K-1}(0,0),...,\pi_{K-1}(S_1,S_2-S_1)\}$$

Then, these stationary probabilities can be obtained as follows: $\mathbf{\Pi} = \mathbf{\Pi Q}$, $\sum_{i=0}^{K-1}\sum_{n_1}\sum_{n_2}\pi_i(n_1,n_2) = 1$

To derive the loss probabilities, it is necessary to determine the probability distribution of the system length ($n_1 + n_2 + 1$, including the server) from the arrival viewpoint, which is equivalent to the steady-state probability distribution $p_i(n_1,n_2)$ [12]. The probabilities must be different from the former departure-point probabilities $\pi_i(n_1,n_2)$, because the state space is enlarged by the state $G = S_2 + 1$, where the "1" accounts for the server. Asymptotically, the number of arriving ATM cells equals the number of departing cells. Hence, the departure rate must be equal to the effective arrival rate of ATM cells which are able to join the system.

$$\begin{aligned}\frac{1-p_i(0,0)}{\Delta t} &= \lambda_i^2\{1-\sum_{n_1+n_2=G}\sum p_i(n_1,n_2)\} \\ &+\lambda_i^1\{1-\sum_{n_2=0}^{S_2-S_1} p_i(S_1+1,n_2) \\ &-\sum_{n_2=0}^{S_2-S_1} p_i(S_1,n_2+1)\frac{1}{S_1+1}\} \quad (10)\end{aligned}$$

where $p_i(n_1,n_2)$ is the steady state probability that an arriving cell sees n_1 RTT cells and n_2 NRTT cells in the system while the MMPP is in state i (i.e., from an arrival point of view)

In general, the arrival point queue length distribution of a single server queue is identical to the departure point queue length distribution, given that arrivals and departures occur singly, i.e., $\pi_i(n_1,n_2)$ is the state probability seen by a cell who joins the queueing system [13][14]. Therefore, the following equation (11) holds for the state probabilities just after a departure.

The following steady-state probabilities can be obtained by combining (10) and (11).

- *for* $n_1 + n_2 \le S_1$ *or* $n_1 < S_1$ *and* $n_1 + n_2 \le S_2$

$$p_i(n_1,n_2) = \frac{\pi_i(n_1,n_2)}{\pi_i(0,0)+\lambda_i\Delta t}$$

- *for* $n_1 = S_1$ *and* $n_1 + n_2 \le S_2$

$$p_i(n_1,n_2) = \frac{\lambda_i}{\lambda_i^2}\frac{\pi_i(n_1,n_2)}{\pi_i(0,0)+\lambda_i\Delta t}$$

- *for* $n_1 + n_2 = G$

$$\begin{aligned}p_i(n_1,n_2) &= 1-\sum_{\{n_1,n_2\}\in B_1}\sum\frac{\pi_i(n_1,n_2)}{\pi_i(0,0)+\lambda_i\Delta t} \\ &-\sum_{\{n_1,n_2\}\in B_2}\sum\frac{\lambda_i}{\lambda_i^2}\frac{\pi_i(n_1,n_2)}{\pi_i(0,0)+\lambda_i\Delta t} \quad (12)\end{aligned}$$

The cell loss probabilities are then given as follows:
a) CLP for NRTT

$$CLP_{NRTT} = \sum_{n_1+n_2=G}\sum p(n_1,n_2). \quad (13)$$

b) CLP for RTT

$$\begin{aligned}CLP_{RTT} &= \sum_{n_2=0}^{S_2-S_1-1} p(n_1 = S_1+1,n_2) \\ &+\sum_{n_2=0}^{S_2-S_1-1} p(n_1 = S_1,n_2+1)\frac{1}{S_1+1} \\ &+CLP_{NRTT}. \quad (14)\end{aligned}$$

3 Performance results

The performance of the SDPI scheme is evaluated for two kinds of traffic classes. We choose source parameters which are characterized by the peak bit rate F_p, the activity factor p, and the mean burst length L_B. Assume that the superposition of such heterogeneous ON-OFF sources are offered to an ATM MUX with the net output link capacity C. The performance of the MUX is evaluated by the queueing model with MMPP source and the SDPI priority scheme. The constant service time of the MUX is given by θ=53 bytes/C. The net link capacity is assumed to be 150Mbps. It is assumed that call arrival rates of two classes of traffics are the same. The source parameters used in our simulations and numerical analysis, which are the same as in [15], are tabulated in Table 1.

Table 1 Source Parameters

class	F_p	p	L_B
RTT	32Kbps	0.35	1400
NRTT	128Kbps	0.1	1600

$$\pi_i(n_1,n_2) = \begin{cases} \dfrac{p_i(n_1,n_2)}{1-\frac{\lambda_i^2}{\lambda_i}\sum\sum_{n_1+n_2=G} p_i(n_1,n_2) - \frac{\lambda_i^1}{\lambda_i}\{\sum_{n_2=0}^{S_2-S_1} p_i(S_1+1,n_2) + \sum_{n_2=0}^{S_2-S_1} p_i(S_1,n_2+1)\frac{1}{S_1+1}\}}, \\ \text{for } n_1+n_2 \le S_1 \text{ or } n_1 < S_1 \text{ and } n_1+n_2 \le S_2 \\ \\ \dfrac{\frac{\lambda_i^2}{\lambda_i} p_i(n_1,n_2)}{1-\frac{\lambda_i^2}{\lambda_i}\sum\sum_{n_1+n_2=G} p_i(n_1,n_2) - \frac{\lambda_i^1}{\lambda_i}\{\sum_{n_2=0}^{S_2-S_1} p_i(S_1+1,n_2) + \sum_{n_2=0}^{S_2-S_1} p_i(S_1,n_2+1)\frac{1}{S_1+1}\}}, \\ \text{for } n_1 = S_1 \text{ and } n_1+n_2 \le S_2 \end{cases} \tag{11}$$

In Fig. 3, cell loss probabilities are plotted as a function of the mean offered load (RTT and NRTT). Note that the simulation results conform to our numerical analysis. The threshold and buffer size are assumed to be 10 and 30, respectively. Fig. 4 shows the comparison between the SDPI and TBD scheme. It is intuitive to see that SDPI achieves the performance improvement for RTT (which is more critical) at the expense of NRTT. As the buffer size increases while holding the threshold fixed, CLPs for RTT remain constant, but CLPs for NRTT decreased. Thus, SDPI outperforms TBD for accommodating RTT, and SDPI may reach comparable performance as TBD for accommodating NRTT by increasing the buffer size.

4 Conclusions

We have studied the cell loss performance of an ATM MUX loaded with a traffic stream from the superposition of multiple ON-OFF sources in the two-class environment using the proposed buffer management scheme. By modeling each type of traffic by a 2-state MMPP, we were able to derive the CLP of the respective traffics (i.e., RTT and NRTT) using the proposed SDPI space priority scheme. This scheme is applicable to schedule delay-tolerant NRTT and delay-sensitive RTT. That is, by delaying the NRTT cells and pushing in the RTT cells selectively, more RTT can be accepted within the acceptable QoS requirement (e.g., CLP). By provisioning additional priority to RTT traffic, SDPI compensate for the disadvantage of threshold-based discarding (TBD) scheme which favors NRTT at an expense of RTT. Thus, channel utilization is improved for RTT by increasing buffer size properly according to this priority mechanism. Simulations have also validated our numerical analysis.

References

[1] G. Hebuterne and A. Gravey, "A Space Priority Queueing Mechanism for Multiplexing ATM Channels," ITC Specialist Seminar, Adelaide, Sept. 1989.

[2] J. Garcia and O. Casals, "Stochastic Models of Space Priority Mechanisms with Markovian Arrival Processes," Annals of Operations Research 35, pp. 271-296, 1992.

[3] H. Kroner and G. Hebuterne, "Priority Management in ATM Switching Nodes," IEEE JSAC, vol. 9, No. 3, pp. 418-427, April 1991.

[4] J-F Chang and C-S Wu, "The Effect of Prioritization of a Concentrator under an Accept, otherwise Reject Strategy," IEEE Trans. Commun., vol. 38, No. 7, pp. 1031-1039, July 1990.

[5] N. Yin and S-Q Li and T. E. Stern, "Congestion Control for Packet Voice by Selective Packet Discarding." IEEE Trans. Commun. vol. 38, no. 5, pp. 674-683, May 1990.

[6] H. Kroner, "Comparative Performance Study of Space Priority Mechanisms for ATM Channel," IEEE INFOCOM'90, San Francisco, pp. 1136-1143, June 1990.

[7] H. Heffes, D. M. Lucantoni, "A Markov Modulated Characterization of Packetized Voice and Data Traffic

and Related Statistical Multiplexer Performance," IEEE JSAC, vol.SAC-4, no. 6, pp. 856-868, Sept. 1986.

[8] R. Nagarajan, J. F. Kurose, D. Towsley, "Approximation Techniques for Computing Packet Loss in Finite-Buffered Voice Multiplexers," IEEE JSAC vol. 9, no. 3, pp. 368-377, April 1991.

[9] A. Baiocchi, N. B. Melazzi, M. Listanti, "Loss Performance Analysis of an ATM Multiplexer Loaded with High Speed ON-OFF Sources," IEEE JSAC, vol. 9, no. 3, pp. 388-393, April 1991.

[10] F. Yegenoglu and B. Jabbari, "Performance Evaluation of MMPP/D/1/K Queues for Aggregate ATM Models," IEEE Proc. INFOCOM'93, pp. 1314-1319, 1993.

[11] S. Kim, M. Lee, M. Kim, "Σ-Matching Technique for MMPP Modeling of Heterogeneous ON-OFF Sources," IEEE Proc. Globecom'94, pp. 1090-1094, 1994.

[12] B. Wolff, "Poisson Arrivals See Time Averages," "Operat. Res., vol. 30, no. 2, pp. 223-231, Apr. 1982.

[13] R. Cooper, "Introduction to Queueing Theory," New York: Macmillan, 1972.

[14] D. Gross, C. M. Harris, "Fundamentals of Queueing Theory," New York: Wiley, 1985.

[15] S. Kowtha, D. Vaman, "A Generalized ATM Model and Its Application in Bandwidth Allocation," IEEE Proc. ICC'92, pp1009-1013, 1992.

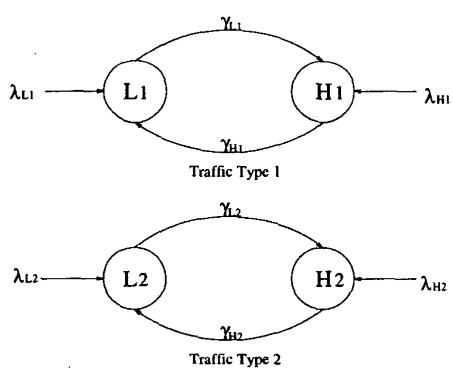

Figure 1. 2-states MMPP models for traffic type 1(RTT) and traffic type 2(NRTT)

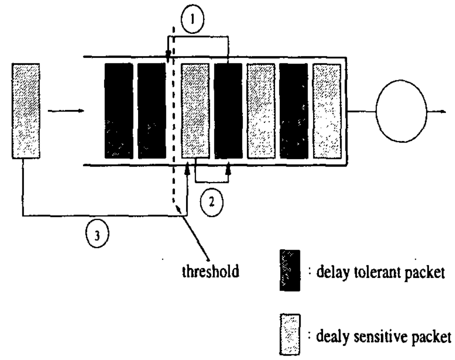

Figure 2. Selective-delay push-in scheme operation

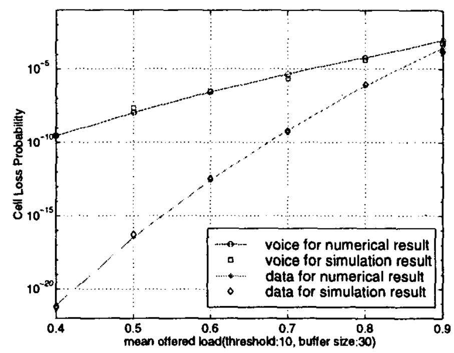

Figure 3. Cell loss probability versus mean offered load (comparison between numerical result and simulation result)

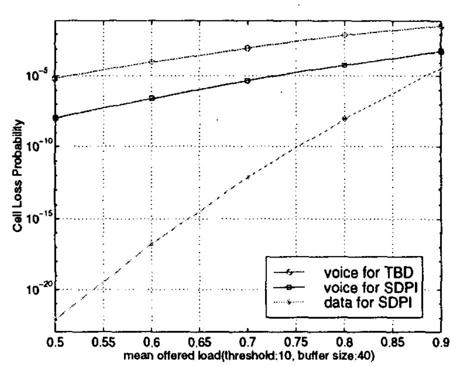

Figure 4. Cell loss probability versus mean offered load (comparison between TBD scheme and SDPI scheme)